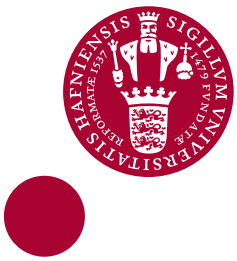

Casein micelles in milk as sticky spheres

Smith, Gregory N.; Brok, Erik; Christiansen, Morten Vormsborg; Ahrné, Lilia

Published in:
Soft Matter

DOI:
10.1039/D0SM01327G

Publication date:
2020

Document version
Peer reviewed version

Soft Matter

ARTICLE TYPE

Cite this: DOI: 00.0000/xxxxxxxxxx

Casein micelles in milk as sticky spheres†

Gregory N. Smith,*[a]§ Erik Brok,[a] Morten Vormsborg Christiansen,[b] and Lilia Ahrné[b]

Received Date
Accepted Date

DOI: 00.0000/xxxxxxxxxx

Milk is a ubiquitous foodstuff and food ingredient, and milk caseins are key to the structural properties of milk during processing and storage. Caseins self-assemble into nanometer-sized colloids, referred to as "micelles", and particles of this size are ideally suited to study by small-angle scattering (SAS). Previous SAS measurements have almost exclusively focussed on the internal structure of the micelles. While important for milk's properties, this attention to the interior of the micelles provides limited information about the structure-forming properties of milk and milk ingredients. The ultra-small-angle X-ray scattering (USAXS) measurements and analysis in this study extend to the micrometer scale, which makes it possible to characterize the interaction between the micelles. Until now, SAS studies have generally excluded a consideration of the interparticle interactions between casein micelles. This is inconsistent with these new data, and it is not possible to model the data without some interparticle attraction. If the micelles are treated as sticky spheres, excellent agreement between experimental data and model fits can be obtained over the length scales studied, from micrometers to ångströms. The stickiness of casein micelles will impact ultra-small-angle scattering and small-angle scattering measurements of casein micelles, but it particularly limits the application of simple approximations, which generally assume that particles are dilute and noninteracting. In summary, this analysis provides an approach to modelling scattering data over many orders of magnitude, which will provide better understanding of interactions between caseins and during food processing.

1 Introduction

Milk is a unique food liquid and is used for the production of various nutritious and delicious food products. Milk transformation into dairy products such as yogurt, cheese, and ice cream highly depends on the interaction properties of the major structure forming components of milk, the "micelles" formed by casein proteins. Besides casein micelles, other milk components such as whey proteins, fat globules, lactose, and mineral content and distribution contribute to the structure formation. Casein, though, is the major component.

Casein micelles are colloidal, self-assembling protein aggregates and constitute the major part of milk proteins of bovine milk (80%), whereas the remaining protein fraction mainly consists of the water-soluble globular whey proteins.[1,2] The microstructure of milk, as result of casein micelle structure and its interactions with other components, is highly influenced by processing and storage conditions, such as temperature, shear, pH, ionic strength, and water content.[3,4] This is important from an industrial perspective since milk microstructure closely relates to the processability and physicochemical and sensory properties of the dairy products, such as firmness, mouthfeel, and spreadability. In some cases, structure build-up of milk proteins may be desirable (such as in yoghurt or cheese), whereas in others it is rather undesirable (such as gelation during ageing of UHT milk). Casein micelles are not perceptibly heat-sensitive, whereas whey proteins readily denature upon heat-treatment leading to binding to casein micelles. In heat-treated milk, denatured, casein-linked whey protein may therefore hinder casein micelle aggregation or alter their physical behavior by water binding and incorporating in casein micelle aggregates, whereas casein micelles may readily coagulate without restriction into larger casein aggregates in unheated milk if the sterically stabilizing κ-casein brush layer is disturbed.[5,6] Small-angle scattering (SAS) is ideally suited for investigations of casein micelles and has, along with other techniques such as microscopy, the potential to contribute to the understanding of the role of milk components in structure formation in dairy products.

Most dairy-related structural studies focus on gel-like dairy products, such as cheese, yogurt, and butter.[7] Regarding liquid milk, most research concerns different variants of heat-treated milk or even reconstituted milk powders.[8–11] In unpasteurized

[a] Niels Bohr Institute, University of Copenhagen, Universitetsparken 5, 2100 Copenhagen Ø, Denmark.
[b] University of Copenhagen, Department of Food Science, 1958 Frederiksberg, Denmark.
† Electronic Supplementary Information (ESI) available: Analysis of published USAXS data. See DOI: 10.1039/cXsm00000x/
§ Present address: ISIS Neutron and Muon Source, Science and Technology Facilities Council, Rutherford Appleton Laboratory, Didcot, OX11 0QX, United Kingdom. E-mail: gregory.smith@stfc.ac.uk

skim milk, however, casein micelles may be able to aggregate differently because of the lower level of denatured whey proteins present. Ultra-small-angle and small-angle scattering (USAS and SAS) methods are powerful methods for non-destructively studying proteins in dispersions. Previously, structure analysis of milk by USAS and SAS has modeled casein micelles as noninteracting spheres or fractal structures.[6,12–14] Much of the previous scattering research on milk and casein have focused on the internal structure of the casein micelles, and various models have been proposed for the arrangement of protein and calcium in the interior. These include a unified power law approach,[12,15–18] multilevel summation of spheres,[19–21] or full model fitting using multiple components.[9,22] Regardless of the approach selected, the casein micelles must be modeled using several contributions, reflecting their hierarchical structure. As this research has been well reviewed elsewhere, it will not be discussed in detail here.[6,23] The salient point from all envisioned structures of casein micelles is that they are spherical colloids that consist of dense and less dense regions in the interior, some of which contain calcium phosphate and some of which contain protein.[20,24,25] Regarding the whole casein micelle colloid, the size of the objects can be determined from scattering data in different ways depending on the specific approach used, either by directly fitting it as sphere for data at sufficiently low Q,[9,13,19,21,22,26] by extrapolation using the Guinier approach (especially when the Stuhrmann approach is used with contrast-variation small-angle neutron scattering experiments)[27], or from the change in power law in a unified fit.[12,15,18]

While less frequently performed than small-angle scattering measurements, ultra-small-angle scattering measurements (using either X-rays, USAXS, or neutrons, USANS) can provide information about the larger length scale structure of dispersions of milk, whether skim milk or fat-containing milk, native milk or reconstituted from powder.[13,17,18,26,28] None of these studies, however, have undertaken detailed model fitting of the entire hierarchy of structures in casein micelle dispersions or adequately fit data over the entire range of length scales. Individual casein micelles or the internal changes that occur during processing can be well described by focussing on the interior of the micelles. However, the structure-forming properties of milk and milk products also arise from the interactions between casein micelles, and between casein and whey proteins, rather than solely from the inner structure of the micelle. Increasing milk viscosity and processing capabilities caused by renneting and gel-formation, for example, depend on protein-protein interactions,[11] on intermicellar rather than intramicellar levels.[29]

In this study, we performed USAXS on unpasteurized skim milk, covering the length scales required to reveal any interactions between casein micelles. This will add to the existing literature about the internal structure of casein micelles[6] by studying the interparticle organization as well. The objective was to find a mathematical model to describe the extent of casein micelle interactions, as these will be influenced by processing and will have consequences for the textural appearance and stability of milk. Rather than just discussing the data qualitatively, we endeavored to find a quantitative model. By using such a mathematical model to quantitatively compare casein micelles, it will be possible to devise metrics to achieve this comparison. As milk is an important ingredient, greater knowledge of casein micelles will be of interest to food scientists. However, these casein structures are colloids that are formed from proteins (biopolymers), and knowledge of protein assembly over long length scales will be of interest to those interested more generally in soft matter.

2 Materials and Methods

2.1 Milk dispersions

Fresh, raw whole milk was collected (Mannerup Møllegård, Lejre, Denmark) and transported to the dairy pilot plant of University of Copenhagen (KU-FOOD, Denmark) for further immediate processing. The milk was continuously heated to the skimming temperature of 55 °C by indirect heating (UHT/HTST Direct & Indirect Processing System, Microthermics, Raleigh, USA) followed by skimming on a pilot scale centrifugal separator (Cream Separator FJ 130 ERR, Milky, Vermont, USA). Despite heating to the desired skimming temperature, the milk was not further heat-treated and is therefore considered "raw" skim milk. The skimmed milk sample for USAXS analysis was loaded directly into a sterilized 7" NMR tube (5 mm diameter, Bruker, MA, USA) and stored at 5 °C until further use (five days). Total solids content of the produced skim milk were determined in triplicate by the ISO 6731:2010 reference method. Total solids content of the skim milk was (9.57 ± 0.06) wt. %, which is consistent with literature.[30–32]

2.2 Ultra-small-angle X-ray scattering (USAXS)

Ultra-small angle X-ray scattering (USAXS) and small angle X-ray scattering (SAXS) experiments were performed using the USAXS Facility at the Advanced Photon Source (APS), Argonne National Laboratory (Lemont, Ill., USA). The instrument is currently located at the beamline APS 9ID. The X-ray energy was 21 keV (wavelength, $\lambda = 0.5895$ Å), and the photon flux was $\sim 5 \times 10^{12}$ mm^{-2} s^{-1}. Samples were measured in 5 mm diameter NMR tubes, and the scattering of water subtracted as background. Full details of the instrument are provided elsewhere.[33–35] Data were reduced, corrected for instrument smearing effects, and placed on an absolute scale using the standard USAXS data processing procedures for the beamline and the Nika software, both packages for Igor Pro.[33,36] Uncertainties in the reduced scattering intensity are not shown in figures as they would be, in general, smaller than the size of the data points. The data at $Q \sim 3 \times 10^{-2}$ Å are noisy because they are in the overlap region between the USAXS and SAXS measurements, and the intensity statistics here are poorest.

The data are presented as the magnitude of the momentum transfer or scattering vector $\vec{Q}$, which is a function of the wavelength (λ) and half the scattering angle (θ).

$$Q = \frac{4\pi \sin\theta}{\lambda} \tag{1}$$

The instrument configuration resulted in a usable Q range (combined USAXS and SAXS) of $3.8 \times 10^{-4} < Q < 2.0 \times 10^{-1}$ Å^{-1}.

The data are modeled using a multilevel model as described in

the text using the SASfit (version 0.94.11) fitting software.[37] Uncertainties from fitting are given. Data are shown as experimental $I(Q)$ versus Q as well as the error-weighted difference function[38] ($\Delta I/\sigma = (I_{exp} - I_{fit})/\sigma$) where I_{exp} and I_{fit} are the experimental and fit scattering intensities, respectively, and σ is the uncertainty of the experimental scattering intensity. The general quality of fits are assessed by considering $\Delta I/\sigma$ over the whole Q range measured as well as by comparing the reduced χ^2 (χ^2_R) of the fit. This parameter is defined as the weighted sum of squares of deviations (χ^2) divided by the degree of freedom (the number of data points and the number of parameters).[39]

3 Results and Discussion

As small-angle scattering has proved so informative to studying, primarily, the internal structure of casein micelles,[6,23] we employ the technique to study the colloidal structure of dispersions of milk as well. Specifically, we use the variant ultra-small-angle scattering, which makes it possible to investigate scattering at lower magnitudes of the momentum transfer or scattering vector $\vec{Q}$ and, consequently, larger length scales. (The magnitude of $\vec{Q}$ is inversely proportional to the length scale d investigated, which can be quantified by Bragg's law as $Q = (2\pi)/d$).[40]

In Figure 1, a literature exemplar of SAXS data on milk dispersions[9] (top, dark blue) are compared to the USAXS and SAXS data presented in this study (bottom, light blue). The two sets of data compare very well, and this shows that the new data that we have obtained here are characteristic of the scattering of milk.[23] There may be differences between milk samples obtained from different origins, but these differences do not reveal themselves in dramatic differences in the scattering data.

The data that we report here, however, does have one important difference. As we have used Bonse–Hart USAXS to study the X-ray scattering of milk dispersions in addition to conventional SAXS, we are able to obtain information about the samples at much longer length scales than in this previous measurement. This provides nearly another order of magnitude to the length scale that we are able to investigate. The modifications that need to be made to describe this data adequately are the subject of the remainder of this paper. These are different ways of including or excluding interactions between the casein micelles, and the sections below are named after the model used for these interactions.

3.1 General casein micelle scattering model

Of the models used for casein micelles posited in the literature, we used the model of Ingham *et al.*[9] (with slight modifications) to fit our data. We favor this model because it balances fitting data over the entire Q range (multiple contributions) with simplicity (cross-terms ignored). This was shown in the original publication to fit the data in the SAXS region well, with support from resonant soft X-ray scattering measurements that were able to identify with certainty the contribution arising from colloidal calcium phosphate.[42] There are four contributions to this model, given below from the largest size to the smallest size.

1. **Casein micelles.** The casein micelles are modeled as homogeneous spheres with a distribution of sizes. The spherical form factor ($P_s(Q)$) depends only on the radius (r) of the spheres.[43]

$$P_s(Q) = \left[\frac{3\left(\sin(Qr) - Qr\cos(Qr)\right)}{(Qr)^3}\right]^2 \quad (2)$$

The distribution of sizes is given by the log-normal function, where the logarithm of a variable (in this case the radius) has a normal distribution. The function is given elsewhere.[39]

2. **Incompressible regions.** The sponge-like incompressible protein regions are fit to a sphere form factor (Equation 2) with a log-normal distribution of radii.[39] We fit both the radius and width of the distribution, unlike in Ingham *et al.*,[9] where they fit only the radius. The ratio of incompressible regions to casein micelles was fixed to 21.96, in accordance with literature.[9]

3. **Colloidal calcium phosphate particles.** The peak at this Q range was shown to be from colloidal calcium phosphate (CCP) by resonant soft X-ray scattering measurements.[42] The CCPs were modeled with a spherical form factor (Equation 2) and a hard sphere structure factor. This structure factor uses the Percus–Yevick closure and the following interparticle interaction potential ($U(h)$, Equation 3), where h

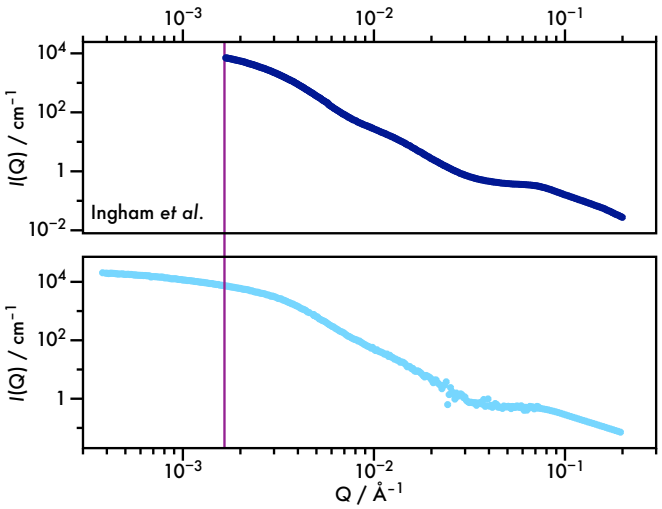

Fig. 1 Example SAXS data from the literature (dark blue, top)[9] and new SAXS/USAXS data (light blue, bottom) for dispersions of milk. The X-ray scattering from milk primarily arises from casein micelles. The data qualitatively appear to be the same, showing that the newly obtained data is consistent with previous measurements. The minimum Q from this previous set of SAXS data[9] is shown as a purple vertical line, and the new USAXS data extend the length scale studied by almost an order of magnitude. (The data from Ingham *et al.* were obtained from the publication using the macOS application GraphClick, which has been shown to be a reliable and viable method to extract data from images.[41] The data were adapted to the plot here. Data adapted from Ingham *et al.*[9] with permission from The Royal Society of Chemistry
)

is the center-center separation.[44,45]

$$U(h) = \begin{cases} \infty & \text{for} \quad h < 2r \\ 0 & \text{for} \quad h \geq 2r \end{cases} \tag{3}$$

The size distribution is accounted for using the local monodisperse approximation, where particles are assumed to always be surrounded by particles of the same size and the scattering scaled according to the size distribution.[46] The CCP radius and the structure factor radius are not equal, and this is due to a layer of protein around the core of the CCPs that prevents them from coming to touch.[6,9,47] This was implemented using a concentric sphere (core with shell) model, with the contrast between the shell and the medium set to 0. The scattering intensity of this contribution is low, and so most of the parameters describing it were fixed. The ratio of CCPs to casein micelles was fixed to 285, in accordance with literature.[6,9,20]

4. **Protein inhomogeneities.** The scattering from polymer chains was modelled differently than Ingham *et al.*,[9] who used a modified Debye–Büche function multiplied by a hard sphere structure factor. In our data, the scattering at high Q varies as a power law proportional to Q^{-2}, which is the signature of a Gaussian polymer chain.[48] The form factor of a Gaussian chain ($P_c(Q)$) depends on the radius of gyration (R_g) of the polymer.

$$P_c(Q) = 2\frac{\exp(-Q^2R_g^2) + Q^2R_g^2 - 1}{Q^4R_g^4} \tag{4}$$

This is then multiplied by a hard sphere structure factor (Equation 3) with a hard sphere radius that is fit and not necessarily equal to R_g. This model gives good agreement with the data we have obtained, despite being found inadequate previously.[9]

Each set of data was fit iteratively to ensure that the number concentration from fitting corresponded to the volume fraction of casein micelles known from the sample preparation. The data were fit initially using the SLD differences calculated by Ingham *et al.*[9] The radii of the casein micelles and their size distribution were used to calculate the volume fraction, which depends on the third moment of the size distribution.[39] This was used to calculate the number concentration, which was then scaled appropriately and fixed, and the SLD differences varied. This process was iterated until the radii and size distributions converged within the certainty of the fit.

3.2 Casein micelles as dilute spheres

In Ingham's model,[9] the casein micelles are treated as dilute spheres, and so the calculated scattering comes from the spherical form factor alone. This equivalently means that the structure factor for the casein micelle contribution is equal to 1. This model was used to fit the newly measured data presented here. The fit was performed over the same Q range as used by Ingham *et al.*[9] (SAXS only). Over this Q range, a similarly good fit can be obtained to that previously reported.

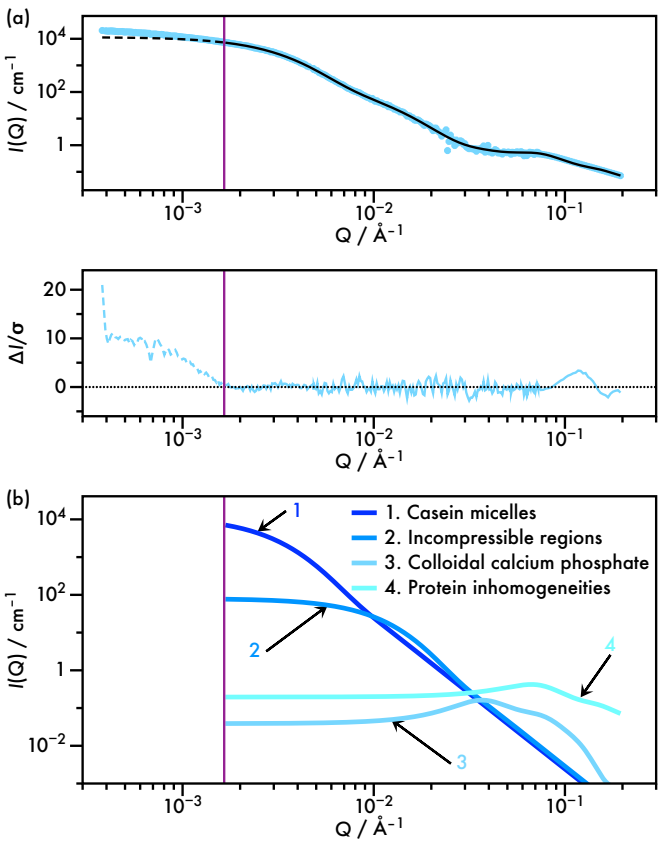

Fig. 2 The USAXS/SAXS data obtained in this study fit to the same minimum Q (vertical purple line) as the data of Ingham *et al.*[9] using the four contribution model explained in the text. The experimental data and model fits ($I(Q)$) and the error-weighted difference function ($\Delta I/\sigma$) are shown in (a). The partial contribution of each component is shown in (b). The different contributions are different colors, which are each numbered and labeled in the legend. The sum of these are represented by a solid black line. Over the SAXS Q range, the fit is very good. The fit data has extended to the USAXS Q range as well, and this is shown by the dashed line. There is poor agreement between the data and the model at the lowest Q that was measured, and this shows that interparticle interactions cannot be ignored when fitting the entire USAXS/SAXS Q range.

Extending this model to lower Q would give a good match to the data if the casein micelles were indeed dilute spheres. At sufficiently low Q, in the Guinier region, the scattering intensity should reach a plateau when $Qr < 1$ and in the absence of interactions.[40] Figure 2 shows this not to be the case. Therefore, additional complexity needs to be added to the model in order to fit scattering data at all length scales. We sought to find a way to describe the spatial distribution of the casein micelles by accounting for a interparticle interactions between the micelles (a structure factor).

3.3 Casein micelles as hard spheres

Because the USAXS data could not be modeled with the casein micelles treated as a dispersion of dilute particles, the complexity of the model was increased by introducing a hard sphere structure

factor to account for excluded volume in a concentrated dispersion. This would enable the data to be fit if the casein micelles experienced only excluded volume effects, without any specific repulsive or attractive interactions.

To reduce the number of fit parameters and to ensure that the structure factor represented reality, the volume fraction of casein micelles was fixed to that known for milk. The concentration of solid material in the milk (9.57 wt. %) was measured experimentally. This was converted to a volume fraction using literature values of the mass proportion of the major components of milk (casein, whey, α-lactose, and β-lactose) for Swedish dairy milk measured in 1995–1996.[49] These are the major components of milk, making up $\sim 90\%$ of the solid material, so the exclusion of the other components is reasonable. The ratio of α to β lactose in milk is known[50,51] and merits considering as the two have different densities. The mass densities of most components (casein, α-lactose, and β-lactose, and water) are known,[52–54] and the density of whey is set to the infinite molar mass asymptotic mass density of a protein.[55] This results in a concentration of 98.6 g L^{-1}, which given the voluminosity of milk (4.4 mL g^{-1}),[56] can be converted to a volume fraction (ϕ) of 0.1400 ± 0.0009. The volume fraction of the casein micelles used for fitting was fixed to this value.

The model then used for fitting was the same as that used when the casein micelles were treated as dilute spheres (with four contributions covering the whole Q range) except for modifying the first (lowest Q) contribution from casein micelles so that they are fit with a hard sphere structure factor ($S(Q)$) rather than with no structure factor. As when a structure factor was used for the CCP, the local monodisperse approximation[46] was used to scale the structure factor to account for the distribution of radii.

A comparison between the casein micelles as hard spheres and the casein micelles as dilute spheres is shown in Figure 3. At high Q, the two are essentially the same, whereas there are small differences between the two at low Q. These differences, however, do not result in a significant improvement in the fit to the data. This shows that the casein micelles cannot be modeled just as noninteracting particles and suggests that there must be some sort of interaction between the micelles, which gives a different spatial distribution of the particles relative to each other and consequently different $S(Q)$. This is only apparent due to the data at low Q that can be obtained by USAXS.

3.4 Casein micelles as sticky spheres

If a hard sphere structure factor applied to the casein micelles cannot fit the data, then the next level of complexity is to introduce interparticle interactions. A decrease in scattering intensity at low Q is a sign of repulsive interactions, whereas an increase in scattering intensity is a sign of attractive interactions.[40] As can be seen in Figures 2 and 3, the scattering intensity at the lowest Q is greater than that predicted by the assuming that the casein micelles are dilute spheres or hard spheres. This shows that the casein micelles are likely to experience attractive interactions. Furthermore, stickiness or attraction between casein micelles has previously been invoked to explain some properties of milk aggregation.[56,57] We use a sticky sphere structure factor to model these intermicelle attractions. Specifically, we use Baxter's model of adhesive spheres.[58] Unlike in the hard sphere case (where the interaction potential is either 0 or infinite, Equation 3), for adhesive spheres, there is a range of interparticle separations (Δ) where the interaction potential is negative. In the Baxter model[58] of adhesive spheres, the pair interaction potential $U(h)$ is now given by Equation 5 (in units of the thermal energy, k_BT).

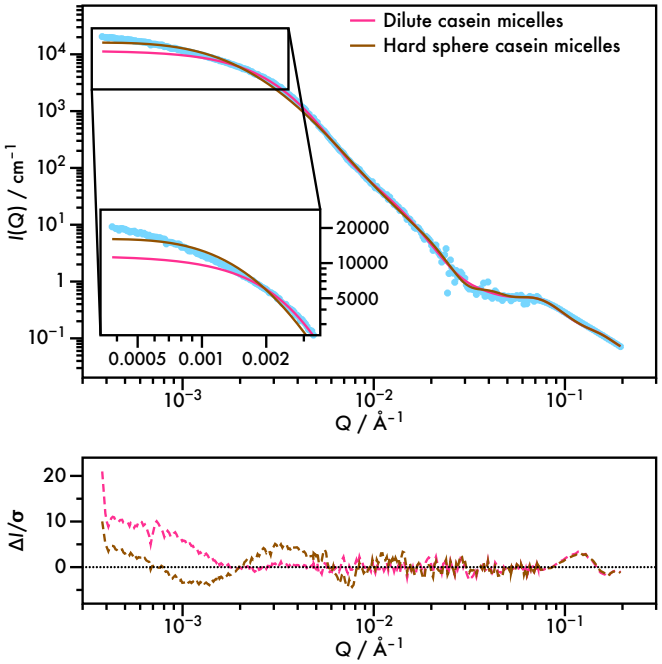

Fig. 3 The USAXS data obtained in this study fit using either the model of Ingham *et al.* where the casein micelles are treated as dilute spheres[9] (extrapolated to the USAXS minimum Q) or a modified version where the casein micelles are treated as hard spheres (using a hard sphere structure factor with the casein micelle contribution). The top panel shows the scattering intensity ($I(Q)$) as a function of Q, and the bottom panel shows the error-weighted difference function[38] ($\Delta I/\sigma$) also as a function of Q. Treating the casein micelles as hard spheres results in a slight improvement over treating them as dilute spheres, but the fit at low Q is still poor. This means that the hard sphere structure factor is not a satisfactory model for the interparticle interactions between the casein micelles and suggests that there are specific interactions between the particles.

$$U(h)/k_BT = \begin{cases} \infty & \text{for} \quad h < 2r \\ \ln\left(\frac{12\tau\Delta}{\sigma+\Delta}\right) & \text{for} \quad 2r < h < 2r+\Delta \\ 0 & \text{for} \quad h > 2r+\Delta \end{cases} \qquad (5)$$

The attraction is then calculated in the limit $\Delta \to 0$.[39] This results in a well that is infinitely deep but infinitesimally narrow.[56] The adhesive strength is quantified by the parameter τ, the stickiness parameter. This model is simple to apply because the attraction between particles is encapsulated in a single parameter, τ. The stickiness parameter can be thought of as a dimensionless measure of the temperature.[58] For comparison with other calculations, τ can be used to calculate the second virial coefficient, B_2. For a given τ, B_2 is equal to $(4-1/\tau)V$, where V is the volume of

the sphere.[57] The model used for fitting was then otherwise the same as when the casein micelles were treated either as dilute spheres or hard spheres. The same four contribution model was used to cover the entire Q range, and the lowest Q contribution (the casein micelles) included the sticky sphere $S(Q)$ described above. A comparison between casein micelles as sticky spheres and casein micelles as dilute spheres is shown in Figure 4. This model gives very good agreement with the data.

The use of Baxter's sticky sphere structure factor is what enables our model to fit the data. The best fit value of τ is 0.165 ± 0.002, which represents fairly sticky spheres. The degree of attraction between spheres increases as τ decreases. For instance, in the limit as $\tau \to \infty$, the sticky sphere interaction potential (Equation 5) reduces to the hard sphere interaction potential (Equation 3).[59] The casein micelles appear to be sticky spheres, but this does not mean that the dispersions are aggregated. From phase diagrams of sticky spheres,[59,60] colloidal dispersions with the particle volume fractions and stickiness parameters of these milk samples are in the nonpercolating fluid phase.[61]

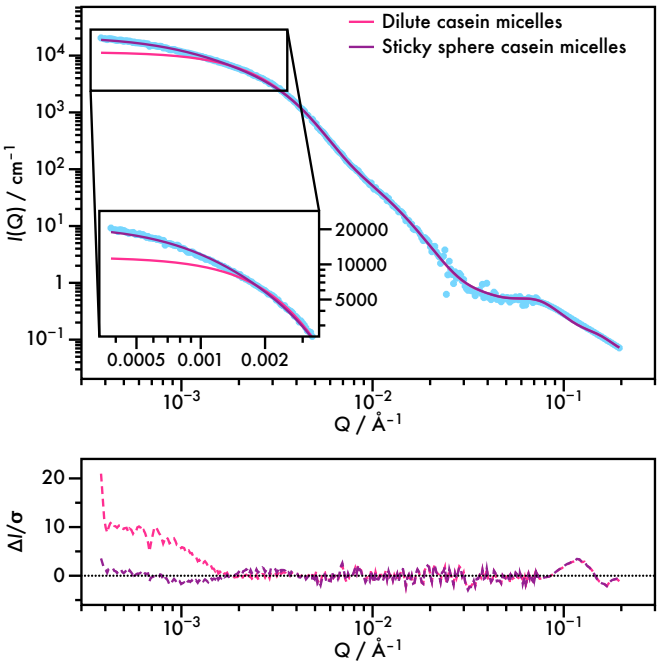

Fig. 4 The USAXS data obtained in this study fit using either the model of Ingham *et al.* where the casein micelles are treated as dilute spheres[9] (extrapolated to the USAXS minimum Q) or a modified version where the casein micelles are treated as sticky (adhesive) spheres (using a sticky sphere $S(Q)$ with the casein micelle contribution). The top panel shows the scattering intensity ($I(Q)$) as a function of Q, and the bottom panel shows the error-weighted difference function[38] ($\Delta I/\sigma$) also as a function of Q. When casein micelles are treated as sticky spheres, there is very good agreement between the fit and the data, which can be seen by the low value of $\Delta I/\sigma$ over the entire Q range. This suggests that a description of the casein micelles as sticky spheres is most consistent with the scattering data.

As far as we are aware, treating casein micelles as sticky spheres has never been necessary to fit scattering data of milk or dispersions of casein micelles previously. For SAXS, this is due to an insufficiently low minimum Q to see the interparticle interactions (Figure 1). For other USAXS data, the increase at low Q was accounted for differently by the groups that measured those data.[12,16–18] We have reanalyzed these literature data using the model presented here, and we find that the model is entirely consistent with the data. (With the proviso that the drastic increase at low Q proportional to power law $Q^{-3.9}$ in the data of of Peyronel *et al.*[18] is considered to be from an object such as residual fat globules or large aggregates rather than from the casein micelles.) These refit literature data are shown in Figures S1 and S2 in the Electronic Supplementary Information.[†]

3.5 Comparing models

In all fits to USAXS data (Figures 2, 3, and 4), the quality of the fit is shown over the entire measured Q range by the error-weighted difference function ($\Delta I/\sigma$). A comparison of this function reveals how good the fit is over all the length scales (equivalently Q) studied. The fits at high Q are similarly good between all the models, but only the model where casein micelles are treated as sticky spheres fits the data well at low Q. Another way to assess the quality of the fit is to consider the magnitude of χ^2_R. Least squares optimization of model fits is built around the hypothesis that the best description of a set of data is the one where the weighted sum of squares of deviations between the data and the fitting functions are minimal.[39]

In Table 1, we show the optimized values of fitting parameters for all three models used in this study. Alongside these values, the goodness of fit (χ^2_R) is shown for all three. As expected from the fits shown in Figures 2, 3, and 4, it is minimal for the model with casein micelles fit as a sticky sphere structure factor.

The merits of the four contribution model that we use to model this data were well discussed when proposed by Ingham *et al.*[9] Our extension of this model to the USAXS regime means that we are able to provide increased certainty over the radius of the casein micelles from model fitting over the entire Q range. The total casein micelle size that we obtain from model fitting using the sticky sphere $S(Q)$ (Table 1), approximately 100 nm in diameter, compares well to values from the literature.[25] This distribution of sizes of casein micelles in milk is broad (also presumably dependent on the source of the milk) and the weighting of the size distribution is also technique dependent. Still, the casein micelle size that we obtain is in general agreement with example sizes obtained from, for instance, small-angle scattering,[12,13,16,18,19,21,22,27] sedimentation,[57] electron microscopy,[15,24] and light scattering.[13,15]

4 Conclusion

As stated previously, bovine casein is important in dairy foods and ingredients due to its unique properties, but it is also a naturally-occurring, self-assembled protein colloid. Physics methodology can be highly relevant and insightful for studying biological, food-relevant materials, and milk is an archetypal material for study.[62,63] Casein is far from the only protein to self-assemble[64], and so knowledge of how to better use tools, such as ultra-small-angle X-ray scattering, to study self-assembly of proteins will be highly valuable to develop novel food processes and products.

Table 1 Best fit parameters for three models presented

	Dilute sphere (no $S(Q)$)	Hard sphere $S(Q)$	Sticky sphere $S(Q)$
Population 1 (Casein micelles) $P(Q)$			
Number density, N_1 / (10^{20} m^{-3})	2.56 ± 0.07	6.4 ± 0.1	1.98 ± 0.05
Median sphere radius, $r_1{}^{\ddagger}$ / Å	425 ± 7	222 ± 3	478 ± 7
Log-normal distribution width parameter, $\sigma_1{}^{\ddagger}$	0.342 ± 0.006	0.52 ± 0.01	0.311 ± 0.006
Volume fraction, ϕ_1	0.139 ± 0.006	0.140 ± 0.005	0.140 ± 0.005
SLD difference, $\Delta\rho_1{}^{\ddagger}$ / (10^{-6} Å^{-2})	0.72 ± 0.01	0.82 ± 0.01	0.79 ± 0.01
Population 1 (Casein micelles) $S(Q)$			
Stickiness parameter, $\tau^{\ddagger}$	—	—	0.165 ± 0.002
Volume fraction, ϕ_1^*	—	0.1400 ± 0.0009	0.1400 ± 0.0009
Population 2 (Incompressible regions)			
Number density, N_2 / (10^{21} m^{-3})	5.6 ± 0.2	14.1 ± 0.3	4.4 ± 0.1
Median sphere radius, $r_2{}^{\ddagger}$ / Å	127 ± 5	135 ± 3	124 ± 6
Log-normal distribution width parameter, $\sigma_2{}^{\ddagger}$	0.31 ± 0.02	0.09 ± 0.03	0.33 ± 0.03
Number per micelle (N_2/N_1)	22.0 ± 0.9	22.0 ± 0.7	22.0 ± 0.8
Proportion of micelle (ϕ_2/ϕ_1)	0.54 ± 0.05	1.07 ± 0.06	0.40 ± 0.04
SLD difference, $\Delta\rho_2{}^{\ddagger}$ / (10^{-6} Å^{-2})	0.57 ± 0.03	0.29 ± 0.01	0.64 ± 0.03
Population 3 (Colloidal calcium phosphate) $P(Q)$			
Number density, N_3 / (10^{22} m^{-3})	7.3 ± 0.2	18.3 ± 0.4	5.6 ± 0.1
Median sphere radius, r_3 / Å	25	25	25
Log-normal distribution width parameter, σ_3	0.15	0.15	0.15
Number per micelle (N_3/N_1)	290 ± 10	285 ± 9	280 ± 10
Proportion of micelle (ϕ_3/ϕ_1)	0.039 ± 0.002	0.097 ± 0.004	0.030 ± 0.001
SLD difference, $\Delta\rho_3{}^{\ddagger}$ / (10^{-6} Å^{-2})	1.9 ± 0.4	1.3 ± 0.3	2.1 ± 0.5
Population 3 (Calcium phosphate) $S(Q)$			
Volume fraction, ϕ_3^*	0.19	0.19	0.19
Population 4 (Protein chains) $P(Q)$			
Intensity scale, $I(Q=0)_4{}^{\ddagger}$ / cm^{-1}	0.7 ± 0.2	0.7 ± 0.2	0.7 ± 0.1
Radius of gyration, $R_{g(4)}{}^{\ddagger}$ / Å	22 ± 3	21 ± 3	22 ± 2
Population 4 (Protein chains) $S(Q)$			
Hard sphere radius, $r_4^{*\ddagger}$ / Å	39.4 ± 0.6	39.0 ± 0.7	39.5 ± 0.6
Volume fraction, $\phi_4^{*\ddagger}$	0.16 ± 0.01	0.15 ± 0.02	0.16 ± 0.01
Goodness of fit			
Reduced χ-square, χ_R^2	15.39	5.66	1.29

‡ Fit parameters.

The primary discovery, and the one with the most impact on studying casein micelles generally, is that casein micelles in unpasteurized skim milk must be treated as an interacting, sticky colloid to successfully model scattering data over all length scales (equivalently over the entire Q range). This has important ramifications on attempting to fit the data, and in particular, the impact of neglecting the structure factor on fitting data. For example, the simple and widely-used Guinier approximation[65] is not valid when there is a structure factor, and if it is used to analyze data, incorrect results are obtained.[66] It will result in an incorrect R_g and extrapolation to $Q = 0$ will not give the correct intensity. Additionally, calculated scale factors will be incorrect if the reduction or increase in scattering intensity arising from structure factor effects is not accounted for. We can see this in Table 1; the SLD differences of the populations are different for the different models. If the model used to describe the data is incomplete, then it is possible that important assumptions or caveats will be overlooked.

To best use scattering data to describe the structure of materials, whether between particles or within particles, measurements need to be performed over all length scales where the sample might have structure. For much of the previous work on casein micelles, this was restricted to the small-angle region[6,9,23] to address the important debate on the internal structure of these species. To fully understand the casein micelle, this region must be extended to the ultra-small-angles (very low Q or equivalently very large length scales). This has been much less frequently done in the literature. In this study, we showed that neglecting to measure and model data from casein micelles in the USAXS region means that there is uncertainty in the model fitting at higher Q as well. This will result in shortcomings in the determined structural parameters of casein micelles. As casein is the structure-forming protein in milk and as stickiness between casein micelles has been postulated be the origin of some of the properties of aggregates of milk, addressing this situation is an important achievement. In this study, we have advanced the understanding of the colloidal structure of casein micelles in milk both by obtaining new data on unpasteurized skim milk in the USAXS region and by showing that it is possible to develop a model that can quantitatively and successfully describe these data over a many orders of magnitude.

Conflicts of interest

There are no conflicts to declare.

Acknowledgements

We thank Jan Ilavsky at the Advanced Photon Source (APS) for support before, during, and after the USAXS measurements and for a careful reading of the manuscript. This research used resources of the Advanced Photon Source, a U.S. Department of Energy (DOE) Office of Science User Facility operated for the DOE Office of Science by Argonne National Laboratory under Contract No. DE-AC02-06CH11357. This work is partly funded by the Innovation Fund Denmark (IFD) as part of project Linking Industry to Neutrons and X-rays (LINX) under File No. 5152-00005B. We thank the Danish Agency for Science, Technology, and Innovation for funding the instrument center DanScatt.

Notes and references

1 Z. Atamer, A. E. Post, T. Schubert, A. Holder, R. M. Boom and J. Hinrichs, *Int. Dairy J.*, 2017, **66**, 115–125.
2 M. Corredig, P. K. Nair, Y. Li, H. Eshpari and Z. Zhao, *J. Dairy Sci.*, 2019, **102**, 4772–4782.
3 E. C. Needs, M. Capellas, A. P. Bland, P. Manoj, D. Macdougal and G. Paul, *J. Dairy Res.*, 2000, **67**, 329–348.
4 J. V. C. Silva, D. Legland, C. Cauty, I. Kolotuev and J. Floury, *Food Hydrocolloids*, 2015, **44**, 360–371.
5 D. J. Oldfield, H. Singh, M. W. Taylor and K. N. Pearce, *Int. Dairy J.*, 1998, **8**, 311–318.
6 C. G. de Kruif, T. Huppertz, V. S. Urban and A. V. Petukhov, *Adv. Colloid Interface Sci.*, 2012, **171–172**, 36–52.
7 A. Tamime, *Structure of Dairy Products*, Blackwell Publishing Ltd, Oxford, 1st edn, 2007.
8 C. R. del Angel and D. G. Dalgleish, *Food Res. Int.*, 2006, **39**, 472–479.
9 B. Ingham, A. Smialowska, G. D. Erlangga, L. Matia-Merino, N. M. Kirby, C. Wang, R. G. Haverkamp and A. J. Carr, *Soft Matter*, 2016, **12**, 6937–6953.
10 S. G. Anema, *Int. Dairy J.*, 2017, **75**, 56–67.
11 J. Singh, S. Prakash, B. Bhandari and N. Bansal, *Food Res. Int.*, 2019, **116**, 103–113.
12 F. Pignon, G. Belina, T. Narayanan, X. Paubel, A. Magnin and G. Gésan-Guiziou, *J. Chem. Phys.*, 2004, **121**, 8138–8146.
13 C. P. Adams, N. Callaghan-Patrachar, F. Peyronel, J. Barker, D. A. Pink and A. G. Marangoni, *Food Struct.*, 2019, **21**, 100120.
14 Y. Wang, B. Eastwood, Z. Yang, L. de Campo, R. Knott, C. Prosser, E. Carpenter and Y. Hemar, *Food Hydrocoll.*, 2019, **96**, 161–170.
15 S. Marchin, J.-L. Putaux, F. Pignon and J. Léonil, *J. Chem. Phys.*, 2007, **126**, 045101.
16 F. Pignon, G. Belina, T. Narayanan, X. Paubel, A. Magnin and G. Gésan-Guiziou, *arXiv*, 2008, arXiv:0812.0879.
17 D. A. Pink, F. Peyronel, B. Quinn and A. G. Marangoni, *Phys. Fluids*, 2019, **31**, 077105.
18 F. Peyronel, A. G. Marangoni and D. A. Pink, *Food Res. Int.*, 2020, **129**, 108846.
19 S. Hansen, R. Bauer, S. B. Lomholt, K. Bruun Quist, J. S. Pedersen and K. Mortensen, *Eur. Biophys. J.*, 1996, **24**, 143–147.
20 A. Bouchoux, G. Gésan-Guiziou, J. Pérez and B. Cabane, *Biophys. J.*, 2010, **99**, 3754–3762.
21 H. Sørensen, J. S. Pedersen, K. Mortensen and R. Ipsen, *Int. Dairy J.*, 2013, **33**, 1–9.
22 A. Shukla, T. Narayanan and D. Zanchi, *Soft Matter*, 2009, **5**, 2884–2888.
23 C. G. De Kruif, *J. Appl. Cryst.*, 2014, **47**, 1479–1489.
24 D. McMahon and B. Oommen, *J. Dairy Sci.*, 2008, **91**, 1709–1721.
25 D. G. Dalgleish, *Soft Matter*, 2011, **7**, 2265–2272.
26 A. J. Jackson and D. J. McGillivray, *Chem. Commun.*, 2011, **47**, 487–489.

27 A. Bouchoux, J. Ventureira, G. Gésan-Guiziou, F. Garnier-Lambrouin, P. Qu, C. Pasquier, S. Pézennec, R. Schweins and B. Cabane, *Soft Matter*, 2015, **11**, 389–399.

28 L. F. van Heijkamp, I. M. de Schepper, M. Strobl, R. H. Tromp, J. R. Heringa and W. G. Bouwman, *J. Phys. Chem. A*, 2010, **114**, 2412–2426.

29 S. G. Sutariya, T. Huppertz and H. A. Patel, *Int. Dairy J.*, 2017, **69**, 19–22.

30 A. Bienvenue, R. Jimenez-Flores and H. Singh, *J. Dairy Sci.*, 2006, **86**, 3813–3821.

31 J. Dumpler and U. Kulozik, *J. Dairy Sci.*, 2015, **49**, 111–117.

32 K. R. Morison, J. P. Phelan and C. G. Bloore, *Int. J. Food Prop.*, 2013, **16**, 882–894.

33 J. Ilavsky, P. R. Jemian, A. J. Allen, F. Zhang, L. E. Levine and G. G. Long, *J. Appl. Cryst.*, 2009, **42**, 469–479.

34 J. Ilavsky, F. Zhang, A. J. Allen, L. E. Levine, P. R. Jemian and G. G. Long, *Metall. Mater. Trans.A*, 2013, **44**, 68–76.

35 J. Ilavsky, F. Zhang, R. N. Andrews, I. Kuzmenko, P. R. Jemian, L. E. Levine and A. J. Allen, *J. Appl. Cryst.*, 2018, **51**, 867–882.

36 J. Ilavsky, *J. Appl. Cryst.*, 2012, **45**, 324–328.

37 I. Breßler, J. Kohlbrecher and A. F. Thünemann, *J. Appl. Cryst.*, 2015, **48**, 1587–1598.

38 J. Trewhella, A. P. Duff, D. Durand, F. Gabel, J. M. Guss, W. A. Hendrickson, G. L. Hura, D. A. Jacques, N. M. Kirby, A. H. Kwan, J. Pérez, L. Pollack, T. M. Ryan, A. Sali, D. Schneidman-Duhovny, T. Schwede, D. I. Svergun, M. Sugiyama, J. A. Tainer, P. Vachette, J. Westbrook and A. E. Whitten, *Acta Crystallogr., Sect. D: Struct. Biol.*, 2017, **73**, 710–728.

39 J. Kohlbrecher, *User guide for the* `SASfit` *software package: A program for fitting elementary structural models to small angle scattering data (April 23, 2020)*, Paul Scherrer Institute, Villigen, Switzerland.

40 I. Grillo, in *Small-Angle Neutron Scattering and Applications in Soft Condensed Matter*, ed. R. Borsali and R. Pecora, Springer Netherlands, Dordrecht, 2008, pp. 723–782.

41 M. A. Boyle, A. L. Samaha, A. M. Rodewald and A. N. Hoffmann, *Comput. Hum. Behav.*, 2013, **29**, 1023–1027.

42 B. Ingham, G. D. Erlangga, A. Smialowska, N. M. Kirby, C. Wang, L. Matia-Merino, R. G. Haverkamp and A. J. Carr, *Soft Matter*, 2015, **11**, 2723–2725.

43 Lord Rayleigh, *Proc. R. Soc. London A*, 1910, **84**, 25–46.

44 J. K. Percus and G. J. Yevick, *Phys. Rev.*, 1958, **110**, 1–13.

45 A. Vrij, *J. Chem. Phys.*, 1979, **71**, 3267–3270.

46 J. S. Pedersen, *J. Appl. Cryst.*, 1994, **27**, 595–608.

47 C. Holt, P. A. Timmins, N. Errington and J. Leaver, *European Journal of Biochemistry*, 1998, **252**, 73–78.

48 B. Hammouda, *Probing Nanoscale Structures—The SANS Toolbox*, `http://www.ncnr.nist.gov/staff/hammouda/the_SANS_toolbox.pdf`.

49 H. Lindmark-Månsson, R. Fondén and H.-E. Pettersson, *Int. Dairy J.*, 2003, **13**, 409–425.

50 P. Zarmpi, T. Flanagan, E. Meehan, J. Mann and N. Fotaki, *Eur. J. Pharm. Biopharm.*, 2017, **111**, 1–15.

51 P. Hiremath, K. Nuguru and V. Agrahari, *Handbook of Pharmaceutical Wet Granulation*, Academic Press, 2019, ch. 8, pp. 263–315.

52 V. H. Holsinger, *V. H. Holsinger*, Van Nostrand Reinhold, New York, 3rd edn, 1988, ch. 6, pp. 279–342.

53 H. Farrell, H. Pessen, E. Brown and T. Kumosinski, *J. Dairy Sci.*, 1990, **73**, 3592–3601.

54 F. E. Jones and G. L. Harris, *J. Res. Natl. Inst. Stand. Technol.*, 1992, **97**, 335–340.

55 H. Fischer, I. Polikarpov and A. F. Craievich, *Protein Sci.*, 2004, **13**, 2825–2828.

56 C. G. de Kruif, *J. Dairy Sci.*, 1998, **81**, 3019–3028.

57 C. G. de Kruif, *J. Colloid Interface Sci.*, 1997, **185**, 19–25.

58 R. J. Baxter, *J. Chem. Phys.*, 1968, **49**, 2770–2774.

59 M. A. Miller and D. Frenkel, *J. Chem. Phys.*, 2004, **121**, 535–545.

60 H. Verduin and J. K. Dhont, *J. Colloid Interface Sci.*, 1995, **172**, 425–437.

61 H. G. Ruis, P. Venema and E. van der Linden, *Food Hydrocoll.*, 2007, **21**, 545–554.

62 A. M. Donald, *Rep. Prog. Phys.*, 1994, **57**, 1081–1135.

63 T. A. Vilgis, *Rep. Prog. Phys.*, 2015, **78**, 124602.

64 J. J. McManus, P. Charbonneau, E. Zaccarelli and N. Asherie, *Curr. Opin. Colloid Interface Sci.*, 2016, **22**, 73–79.

65 A. Guinier and G. Fournet, *Small-Angle Scattering of X-Rays*, John Wiley & Sons, New York, 1955.

66 A. V. Smirnov, I. N. Deryabin and B. A. Fedorov, *J. Appl. Cryst.*, 2015, **48**, 1089–1093.